

Modeling and optimizing the temperature distribution around cancerous tissues during magnetic hyperthermia treatment

Mehdi Kohani, Masoud Talebi, Mohammad Behshad Shafii

Department of Mechanical Engineering, Sharif University of Technology, Tehran Iran

Abstract - In magnetic nanoparticle hyperthermia treatment, the ideal objective is to destroy all tumor cells without any damage to neighboring normal tissues. Thus, the temperature distribution in cancerous tissue and also surrounding healthy tissues should become closer to the desired distribution. In this paper, the temperature distribution is estimated by using a numerical scheme to solve the Penne's bioheat transfer equation in a bi-layered spherical tissue with blood perfusion and metabolism. The accuracy of the present model was justified by comparing with an experimental data and similar analytical schemes. Changing the parameters of cancerous tissue showed that the most effective parameter, to optimize the treatment, is the tissue conductivity. Subsequently, we demonstrated that among different factors influencing the tissue conductivity, the mass fraction of water in the tissue is the main factor. According to mass fraction of water in cancerous tissue, two methods of magnetic nanoparticle hyperthermia treatment was suggested.

Keywords: Penne's Bioheat transfer equation, Magnetic Nanoparticle Hyperthermia, Bi-layered solid sphere

1. Introduction

Magnetic fluid hyperthermia is a new method of cancer treatment. In the realm of oncology therapeutics, hyperthermia is a general term for increasing the temperature of tissue above the physiologic level (40°C to 45°C) within a targeted tumor without damaging the surrounding healthy tissue. [1]

During magnetic hyperthermia treatment, the drug which contains magnetic nanoparticles is injected into the patient's body. Thus, by using an alternating magnetic field near the tumor site, not only does drug absorption increase near cancerous cells, but also heat is produced and adjacent cells are ablated because of hysteresis effects. The underlying mechanism that dominates this type of heating results from the production of (electric) eddy currents. These currents produce heat that scales as:

$$SAR_{EC} \propto f^2 \cdot H^2 \cdot r^2$$

Where SAR is the tissue-specific absorption rate, measured as W/g tissue, r is the radius of exposed region, and f and H are the AMF frequency and amplitude, respectively. [2]

Andrä et al. [3] modeled small breast carcinomas surrounded by extended healthy tissue as a solid sphere with constant heat generation caused by FePt magnetic nanoparticles (MNPs), and measured the temperature distribution.

Maenosono and Saita [6] and Lin & Liu [5] used FePt magnetic nanoparticles (MNPs) for magnetic hyperthermia and estimate the temperature distribution by using numerical approaches to solve Penne's bio-heat equation.

As one of the current obstacles in using this method is that surrounding tissue is also affected or ablated by heat, this method will be optimized when the heat produced by metallic compounds only affects tumor tissue. Therefore, a mechanism must be introduced to minimize the susceptibility of surrounding tissue to heat. This will be possible when the temperature distribution in tumor tissue is ideal. In order to do this, a model is needed to approximate the temperature distribution in tumor and surrounding normal tissues. Because of the sensitivity of healthy cells to temperature fluctuation, the accuracy of this model is critical to obtain reliable results.

In this paper we introduce a modified model that uses a new numerical approach to obtain the inverse Laplace transform of Penne's bio-heat equation. The estimated results are compared with those in the literature [3, 5, 6]. These comparisons show that the present model has a better accuracy than other numerical approaches. Base on this model, we compare the effect of changing three main parameters to determine the most critical one which is conductivity. Subsequently, we found that the most important parameter in conductivity is the mass fraction of water in the tissue. Finally with respect to our results some suggestions were made to optimize the temperature distribution by changing effective parameters.

2. Material and methods

To simplify the problem, we assume the tumor to be a spherical tissue with radius R, and the surrounding normal tissue to be a bigger concentric sphere with radius a. We also make the assumption that nanoparticles absorb homogeneously only into the tumor tissue. As the result of homogeneity, all thermodynamic parameters in the tissues are constant. By alternating the magnetic field, a constant power density will be produced in the tumor tissue due to hysteresis losses. This power density is denoted by P which is directly related to the SAR value. This power produces a temperature distribution in both the tumor and normal tissue as a function of time (t) and radius (r). Now, by employing the heat transfer equation the temperature distribution in tissues can be obtained.

Regarding the spherical shape of tumor tissue, a shell spherical control volume can be assumed. By using the heat transfer equation in spherical coordinates, the following equations are obtained:

$$\begin{aligned} \frac{\partial}{\partial t}(\rho c T) &= \text{div}(k \cdot \text{grad}(T)) + \text{generation} + \text{convection} \\ \rho c \frac{\partial T}{\partial t} &= k \frac{1}{r^2} \frac{\partial}{\partial r} \left(r^2 \frac{\partial T}{\partial r} \right) + q_m + p + ? \end{aligned} \quad (1)$$

In the equation above, convection heat transfer is unknown. This quantity can be approximated by assuming quasi-steady state conditions and applying the first law of thermodynamics:

$$\dot{m}(h_i - h_e) + \dot{Q}_c - \dot{W} = \frac{\partial E}{\partial t} \quad (2)$$

$$\dot{Q}_c = \dot{m}(h_i - h_e) = \dot{m}c(T_i - T_e) = \rho_b c_b w_b (T_i - T_e) \quad (3)$$

Equations 1 and 3 lead to Penne's bioheat equation, formulated in equations 4 and 5 below:

$$\rho_1 c_1 \frac{\partial T_1}{\partial t} = k_1 \frac{1}{r^2} \frac{\partial}{\partial r} \left(r^2 \frac{\partial T_1}{\partial r} \right) + \rho_b c_b w_{b1} (T_b - T_1) + q_{m1} + p \text{ for } r \leq R \quad (4)$$

$$\rho_2 c_2 \frac{\partial T_2}{\partial t} = k_2 \frac{1}{r^2} \frac{\partial}{\partial r} \left(r^2 \frac{\partial T_2}{\partial r} \right) + \rho_b c_b w_{b2} (T_b - T_2) + q_{m2} \text{ for } R \leq r \leq a \quad (5)$$

The various parameters in these equations are defined as follows:

(The subscript "1" refers to tumor tissue, while the subscript "2" refers to normal tissue)

T represents the temperature.

ρ is the density.

c is the specific heat capacity.

k is the thermal conductivity.

T_b represents the blood temperature far from cancerous tissue.

q is the metabolic heat generation rate.

P is the heat generated by magnetic nanoparticles at the tumor site.

w_b is the blood perfusion rate.

Following equations are applied for initial and boundary conditions [5]:

Spherical symmetry:

$$T_1(0, t) \text{ is finite} \quad (6)$$

Continuity of temperature at the interface:

$$T_1(R, t) = T_2(R, t) \quad (7)$$

Thermal energy conservation:

$$K_1 \frac{\partial T_1(R, t)}{\partial r} = K_2 \frac{\partial T_2(R, t)}{\partial r} \quad (8)$$

Heat flux rate at the edge of surrounding normal tissues

$$\frac{\partial T_2(a, t)}{\partial r} = 0 \quad (9)$$

The initial conditions become (j= 1, 2):

$$T_j(r, 0) = T_0 \quad (10)$$

$$\frac{\partial T_j(r, 0)}{\partial t} = 0 \quad (11)$$

$$q_j(r, 0) = 0 \quad (12)$$

A new dependent variable, H, is defined as:

$$H = r(T - T_0) \quad (13)$$

Therefore the initial and boundary conditions are rewritten as:

$$H_1(0, t) = 0 \quad (14)$$

$$H_1(R, t) = H_2(R, t) \quad (15)$$

$$K_1 \left[\frac{\partial H_1(R, t)}{\partial r} - \frac{H_1}{R} \right] = K_2 \left[\frac{\partial H_2(R, t)}{\partial r} - \frac{H_2}{R} \right] \quad (16)$$

$$\frac{\partial H_2(a, t)}{\partial r} - \frac{H_2}{a} = 0 \quad (17)$$

$$\frac{\partial H_j(r, 0)}{\partial t} = 0 \quad (18)$$

$$q_j(r, 0) = 0 \quad (19)$$

Applying the Laplace transform to the equations above with respect to time (t), the initial and boundary conditions can be rewritten as:

$$\frac{d^2 \widetilde{H}_j}{dr^2} - \gamma^2 \widetilde{H}_j = -f_j r \quad (20)$$

$$\widetilde{H}_1(0, s) = 0 \quad (21)$$

$$\widetilde{H}_1(R, s) = \widetilde{H}_2(R, s) \quad (22)$$

$$K_1 \left[\frac{\partial \widetilde{H}_1(R, s)}{\partial r} - \frac{\widetilde{H}_1}{R} \right] = K_2 \left[\frac{\partial \widetilde{H}_2(R, s)}{\partial r} - \frac{\widetilde{H}_2}{R} \right] \quad (23)$$

$$\frac{\partial \widetilde{H}_2(a, s)}{\partial r} - \frac{\widetilde{H}_2}{a} = 0 \quad (24)$$

$$\gamma_j^2 = \frac{1}{K_j} (\rho_j c_j s + \rho_b c_b w_b) \quad (25)$$

$$f_1 = \frac{q_{m1} + p}{k_{1s}} \quad (26)$$

$$f_2 = \frac{q_{m2}}{k_{2s}} \quad (27)$$

The initial and boundary conditions used in the equations above give the following solution:

$$\widetilde{H}_1 = C_1 (e^{\gamma_1 r} - e^{-\gamma_1 r}) + r \frac{f_1}{\gamma_1^2} \quad (28)$$

$$\widetilde{H}_2 = C_2 \left(\frac{a\gamma_2 + 1}{a\gamma_2 - 1} e^{\gamma_2(r-2a)} - e^{-\gamma_2 r} \right) + r \frac{f_2}{\gamma_2^2} \quad (29)$$

Where constants are as:

$$N_0 = \frac{(a\gamma_1 + 1)}{(a\gamma_1 - 1)} e^{\gamma_1(R-2a)} - e^{-\gamma_1 R} \quad (30)$$

$$N_1 = \frac{(e^{\gamma_1 R} - e^{-\gamma_1 R})}{N_0} \quad (31)$$

$$N_2 = \frac{\left(\frac{f_1}{\gamma_1^2} - \frac{f_2}{\gamma_2^2} \right) R}{N_0} \quad (32)$$

$$N_3 = \frac{(a\gamma_2 + 1)}{(a\gamma_2 - 1)} e^{\gamma_2(R-2a)} - e^{-\gamma_2 R} \quad (33)$$

$$N_4 = K_1 \gamma_1 (e^{\gamma_1 R} - e^{-\gamma_1 R}) + \frac{K_2 - K_1}{R} (e^{\gamma_1 R} + e^{-\gamma_1 R}) + K_2 \gamma_2 N_1 N_3 \quad (34)$$

$$N_5 = K_2 \gamma_2 N_2 N_3 - K_2 \left(\frac{f_1}{\gamma_1^2} - \frac{f_2}{\gamma_2^2} \right) \quad (35)$$

$$C_1 = \frac{N_5}{N_4} \quad (36)$$

$$C_2 = N_1 C_1 + N_2 \quad (37)$$

Therefore, the inverse Laplace transform yields the temperature distribution function H, which cannot be obtained analytically. Thus, the numerical solution presented by J. Abate and P. P. Valko [7] is applied to this problem, which gives an approximate result for the function H.

The accuracy of this method can be determined as [7]:

$$\left| \frac{f(t) - f(t, M)}{f(t)} \right| \approx 10^{-0.6M} \quad (38)$$

M is the number of precision decimal digits which is assumed to be three in this article.

Using above method, the function H can be approximated as:

$$H(t, M) = \frac{r}{M} \left\{ \frac{1}{2} \widetilde{H}(r) e^{rt} + \sum_{k=1}^{M-1} \text{Re} \left[e^{ts(\theta_k)} \widetilde{H}(s(\theta_k)) (+i\sigma(\theta_k)) \right] \right\} \quad (39)$$

$$s(\theta) = r\theta(\cot \theta + i) \quad -\pi < \theta < \pi \quad (40)$$

$$\sigma(\theta) = \theta + (\theta \cot \theta - 1) \cot \theta \quad (41)$$

$$r = \frac{2M}{5t} \quad (42)$$

By calculating H from equation (40) and using equation (13), the temperature in the tumor will be obtained, at every radius r and at every time t.

3. Results and discussion

The thermal effects of nanoparticle-injected (FePt) tissues, was demonstrated by Maenosono & Saita [6]. In this research work, parameters of the table 3.1 and table 3.2 were used.

Table3.1. Dimensions of tissues and properties of magnetic field used by Maenosono & Saita [6]

Radius of tumor tissue	R=5mm
Radius of normal tissue	a=15mm
The magnetic field's amplitude	5mT
The magnetic field's frequency	300kHz

Table3.2. Heat produced by magnetic nanoparticles [6]

Type of magnetic nanoparticles	9-nm FePt FCC	19-nm magnetite
Heat Generation	$P_1=3.97 \times 10^5 \frac{W}{m^3}$	$P_2=1.95 \times 10^5 \frac{W}{m^3}$

Figure (1) shows the temperature distribution at t=600s for P₁ and P₂ as a function of distance from the center of the tumor.

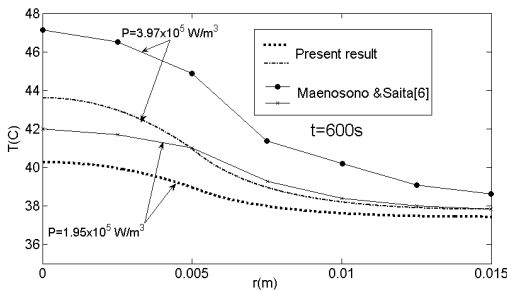


Figure 1. Temperature distributions in the finite tissue at t=600s, for $P_1=3.97 \times 10^5 \text{ W/m}^3$ (9-nm fcc FePt MNP s) and $P_2=1.95 \times 10^5 \text{ W/m}^3$ (19-nm magnetite MNPs)

Here the diagram is compared with the results of Maenosono & Saita [6]. Obviously, since Maenosono & Saita [6] used far less data points, we can conclude that our results have improved accuracy. Moreover, it is demonstrated in figure (1) that the temperature distribution in the tumor tissue ($r < 0.005\text{m}$) is approximately linear. This is in complete contradiction with the nature of heat transfer in that region. Due to heat generation in tumor tissue by the nanoparticles, the temperature distribution must be parabolic which agrees with present results.

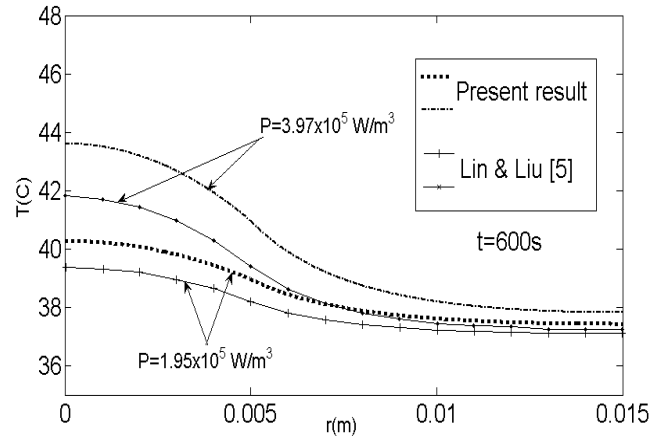


Figure 2. Temperature distributions in the finite tissue at t=600 s for $P_1=3.97 \times 10^5 \text{ W/m}^3$ (9-nm fcc FePt MNPs) and $P_2=1.95 \times 10^5 \text{ W/m}^3$ (19-nm magnetite MNPs)

Figure (2) show that the present results are in better agreement with the curves presented by Lin & Liu [5].

In order to confirm the accuracy of the present approach, it is necessary to compare the present results of temperature distribution with experimental results. The temperature distribution of the tumor and neighboring normal tissue is calculated using parameter values given by Andra et al. [3], and it is compared with experimental results in figure (3). It should be mentioned that although Andra et al. [3] and Lin & Liu [5] used the same parameters, they differ in value.

According to figure (3), the analytical results are in good agreement with the experimental results obtained by Andra et al. [3]. Therefore, the method presented in our work is a reliable means of modeling the temperature distribution in cancerous and normal tissue.

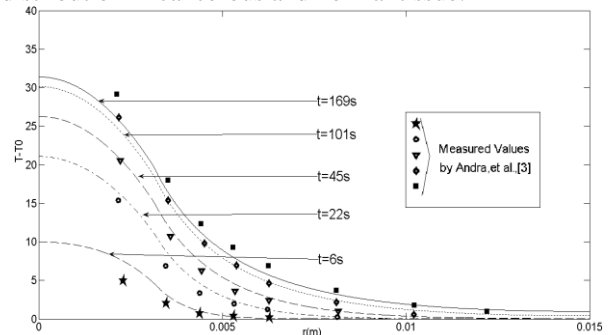


Figure 3. Temperature distribution as a function of the distance from the center of the tumor for different exposure times, using the parameters given in [3]. Measured values for the same parameters are plotted with symbols.

The present distribution curve can be converged to that of the ideal condition by changing the effective parameters

of normal and cancerous tissue. This necessitates the knowledge of the effect that each of these parameters has on the temperature distribution.

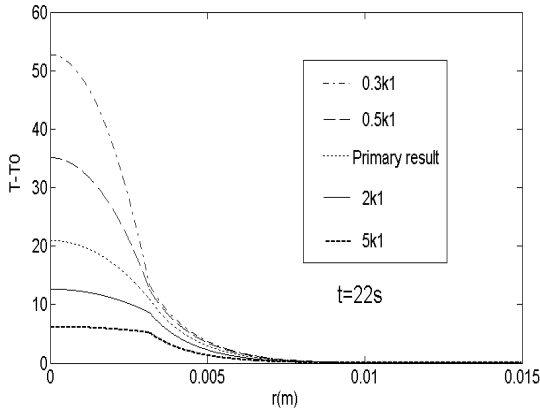


Figure 4. Temperature distribution variation for different values of k_1 (heat conductivity of tumor tissue) calculated at $t=22s$.

Different curves of temperature distribution with different values of parameters (k_1 , c_1 , w_{b1}) are compared in figures (4), (5), (6) (all calculated at $t=22s$). It should be noted that c_2 and k_2 are the normal tissue parameters and it is obvious that changing these parameters is not as easy as changing the tumor tissue parameters.

In figure (4), the temperature distribution converges to the ideal condition as k_1 is reduced.

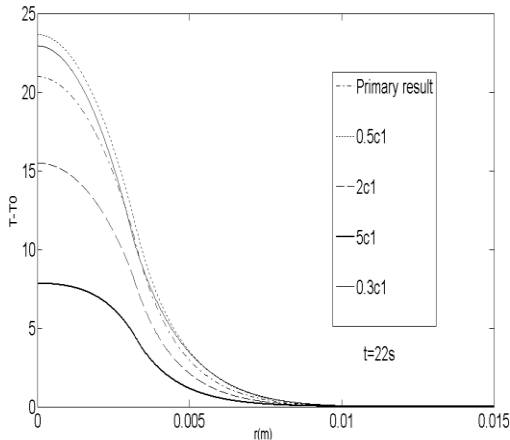


Figure 5. Temperature distribution variation for different values of c_1 (specific heat capacity of tumor tissue) calculated at $t=22s$.

Figure (5) shows that the temperature of the center of tumor decreases with increasing c_1 .

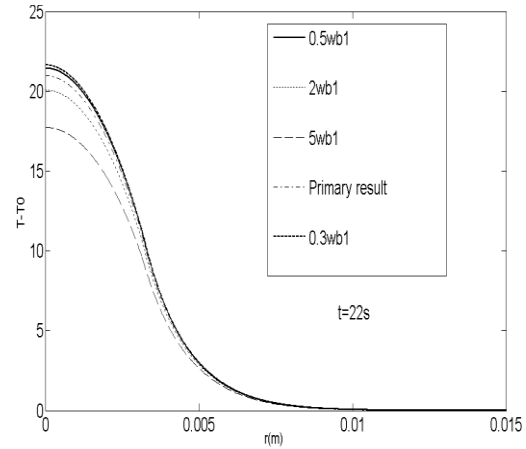


Figure 6. Temperature distribution variation for different values of w_{b1} (blood flow rate in tumor tissue), calculated at $t=22s$.

Figure (6) shows that temperature distribution is less sensitive to w_{b1} variation as compared to c_1 & k_1 . It seems that decreasing human activity, resulting in less blood flow rate, can enhance this therapy. The reason is that decreasing blood flow rate leads to less convection heat transfer, and so heat generated by nanoparticles would not be transferred through the bloodstream.

Summarizing the results of figures (4), (5) and (6), it can be concluded that the temperature distribution at the tumor site is mostly affected by the heat conductivity of the tumor tissue, among other factors. This can also be inferred from boundary condition (9). Therefore to achieve ideal temperature distribution, the most effective way is to reduce k_1 .

From the knowledge of heat transfer principles, it is obvious that large values of conductivity make the temperature distribution uniform and small values make a large temperature gradient. Therefore it could be concluded that, there are two methods in magnetic nanoparticle hyperthermia. The first is to destroy all tumor tissue, while also destroying nearby normal tissue cells, by increasing conductivity of the tumor tissue. The second is to completely destroy the center of the tumor with incurring less damage to normal tissues by decreasing conductivity of the tumor tissue. The best treatment is a choice that would have to be made by the physician.

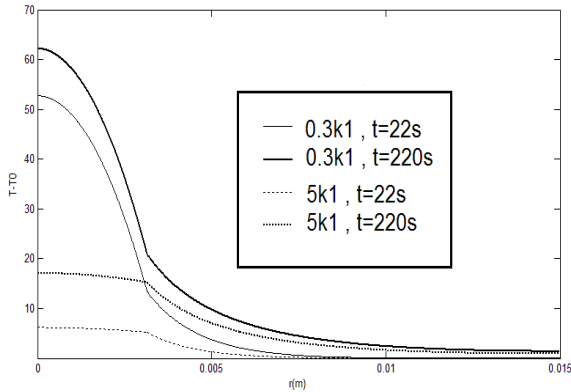


Figure 7. Temperature distribution for conductivity value equal to $0.3k_1$ and $5k_1$ at $t=22s$ and $t=220s$, where k_1 is the conductivity of the cancerous tissues given by Andra et al. [3].

Fig (7) shows the temperature distribution for conductivity value equal to $0.3k_1$ and $5k_1$ at $t=22s$ and $t=220s$. This figure illustrates the two suggested method of magnetic hyperthermia treatment therapy.

Conductivity of biological tissues (k) depends on various parameters such as water content percentage, the amount of fat and protein [8], and temperature [9].

Noting the first assumption in solving Penne's equation which states that conductivity is independent of temperature, variation of K should be measured based on changing water and fat and protein content, only.

According to Cooper and Trezck [9], the following relation holds between these parameters:

$$k(mW/cm - ^\circ C) = \rho \sum_n \frac{k_n m_n}{\rho_n} = \rho(6.28m_{water} + 1.17m_{protein} + 2.3m_{fat}) \quad (43)$$

Based on equation (43), it seems that changing the water content of a tissue is more effective than changing fat or protein content because its coefficient is greater than others. Thus it is possible to obtain different temperature distributions based on different water contents in order to draw closer to our ideal temperature distribution.

4. Conclusion

A numerical solution has been introduced in this paper in order to obtain temperature distribution in tumor tissue treated with magnetic nanoparticle hyperthermia. Based on the proposed method of calculation, the results were very close to experimental curves. These results are reliable as they are close to other numerical results in

literature [5, 6], as well as experimental measurements [3]. Some factors that affect thermodynamic parameters of the tissue are presented in this article and their relative effects are shown in various figures. According to these figures, the best way to obtain optimal distribution is to reduce conductivity of the tumor tissue by increasing its water content. Also, two methods of magnetic nanoparticle hyperthermia treatment based on conductivity value were suggested.

5. References

- [1] G.F. Goya, V. Grazu and M.R. Ibarra: Current Nanosci. 4 (2008) 1.
- [2] Ivkov R., DeNardo S., et al. Application of High Amplitude Alternating Magnetic Fields for Heat Induction of Nanoparticles Localized in Cancer. Clin Cancer Res 2005; 11 (19 Supply): 7093s.
- [3] Andra W, d'Ambly C G, Hergt R, Hilger I and Kaiser W A 1999 Temperature distribution as function of time around a small spherical heat source of local magnetic hyperthermia Journal of Magnetism and Magnetic Materials 194 197-203.
- [4] N. Tsuda, K. Kuroda, Y. Suzuki, An inverse method to optimize heating conditions in RF-capacitive hyperthermia, IEEE Trans. Biomed. Eng. 43 (1996) 1029–1037.
- [5] Chin-Tse Lin, Kuo-Chi Liu, Estimation for the heating effect of magnetic nanoparticles in perfused tissues, International Communications in Heat and Mass Transfer 36 (2009) 241–244.
- [6] S. Maenosono, S. Saita, Theoretical assessment of FePt nanoparticles as heating elements for magnetic hyperthermia, IEEE Trans. Magn. 42 (2006) 1638–1642.
- [7] Abate J. and P. P. Valko. 2004. Multi-precision Laplace inversion. Int. J. Numer. Meth. Engng. 60, 979-993.
- [8] Valvano, J.W., Badeau, A.F., and Pearce, J.A., 1987, "Simultaneous Measurement of Intrinsic and Effective Thermal Conductivity", Heat Transfer in Bioengineering and Medicine, ASME Winter Annual Mtg., Boston, HTD Vol. 95, BED Vol. 7, ed. Chato, Diller, Diller, Roemer, pp. 31-36.
- [9] Cooper, T.E., and Trezck, G.J. Correlation of thermal properties of some human tissues with water content, Aerospace. Med., 42, 24–27, 1971.